



HAL
open science

Saturation-excess overland flow in the European loess belt: An underestimated process?

Valentin Landemaine, Olivier Cerdan, Thomas Grangeon, Rosalie Vandromme, Benoît B. Laignel, Olivier Evrard, Sébastien Salvador-Blanes, Patrick Laceby

► To cite this version:

Valentin Landemaine, Olivier Cerdan, Thomas Grangeon, Rosalie Vandromme, Benoît B. Laignel, et al.. Saturation-excess overland flow in the European loess belt: An underestimated process?. International Soil and Water Conservation Research, 2023, 11 (4), pp.688-699. 10.1016/j.iswcr.2023.03.004 . hal-04067779v1

HAL Id: hal-04067779

<https://hal.science/hal-04067779v1>

Submitted on 13 Apr 2023 (v1), last revised 24 Oct 2023 (v2)

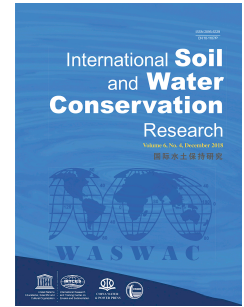
HAL is a multi-disciplinary open access archive for the deposit and dissemination of scientific research documents, whether they are published or not. The documents may come from teaching and research institutions in France or abroad, or from public or private research centers.

L'archive ouverte pluridisciplinaire **HAL**, est destinée au dépôt et à la diffusion de documents scientifiques de niveau recherche, publiés ou non, émanant des établissements d'enseignement et de recherche français ou étrangers, des laboratoires publics ou privés.

Journal Pre-proof

Saturation-excess overland flow in the European loess belt: An underestimated process?

Valentin Landemaine, Olivier Cerdan, Thomas Grangeon, Rosalie Vandromme, Benoit Laignel, Olivier Evrard, Sébastien Salvador-Blanes, Patrick Laceyby



PII: S2095-6339(23)00025-4

DOI: <https://doi.org/10.1016/j.iswcr.2023.03.004>

Reference: ISWCR 404

To appear in: *International Soil and Water Conservation Research*

Received Date: 11 October 2022

Revised Date: 21 March 2023

Accepted Date: 27 March 2023

Please cite this article as: Landemaine V., Cerdan O., Grangeon T., Vandromme R., Laignel B., Evrard O., Salvador-Blanes Sé. & Laceyby P., Saturation-excess overland flow in the European loess belt: An underestimated process?, *International Soil and Water Conservation Research* (2023), doi: <https://doi.org/10.1016/j.iswcr.2023.03.004>.

This is a PDF file of an article that has undergone enhancements after acceptance, such as the addition of a cover page and metadata, and formatting for readability, but it is not yet the definitive version of record. This version will undergo additional copyediting, typesetting and review before it is published in its final form, but we are providing this version to give early visibility of the article. Please note that, during the production process, errors may be discovered which could affect the content, and all legal disclaimers that apply to the journal pertain.

© 2023 International Research and Training Center on Erosion and Sedimentation, China Water and Power Press, and China Institute of Water Resources and Hydropower Research. Publishing services by Elsevier B.V. on behalf of KeAi Communications Co. Ltd.

1 **Saturation-excess overland flow in the European loess**
2 **belt: An underestimated process?**

3 Valentin Landemaine (1), Olivier Cerdan (1), Thomas Grangeon (1), Rosalie Vandromme
4 (1), Benoit Laignel (2), Olivier Evrard (3), Sébastien Salvador-Blanes (4), and Patrick
5 Laceby (5)

6
7 (1) BRGM, F-45060 Orléans, France.

8 (2) University of Rouen, M2C, Rouen, France.

9 (3) Laboratoire des Sciences du Climat et de l'Environnement (LSCE/IPSL), Unité Mixte
10 de Recherche 8212 (CEA/CNRS/UVSQ), Université Paris-Saclay, Gif-sur-Yvette, France.

11 (4) University of Tours, EA 6293 – Géo-hydrosystèmes continentaux (GEHCO), France.

12 (5) Environmental Monitoring and Science Division, Alberta Environment and Parks,
13 Calgary, Alberta, Canada.

14

15 Corresponding author: Cerdan Olivier, o.cerdan@brgm.fr

16

1 **Saturation-excess overland flow in the European loess** 2 **belt: An underestimated process?**

3 4 **Abstract**

5 A major challenge in runoff and soil erosion modelling is the adequate representation of
6 the most relevant processes in models while avoiding over parameterization. In the
7 European loess belt, progressive soil crusting during rainfall events, resulting in
8 infiltration-excess runoff, is usually considered the dominant process generating runoff
9 on catchments covered with silty soils. Saturation-excess may also occur and affect their
10 runoff and erosion behavior. However, saturation-excess runoff occurrence and
11 quantification have rarely been performed and is usually not taken into account when
12 modelling runoff and erosion in these environments. Accordingly, a continuous
13 simulation of the Austreberthe catchment (214 km²), located in the European loess belt
14 (Normandy, France), was conducted with the new Water and Sediment (WaterSed)
15 model over 12 years, corresponding to more than 780 individual rainfall events, at a 25
16 m spatial resolution.

17 The inter-annual variability of runoff and erosion was closely linked to the number of
18 intense events per year and their distribution through the year. The model was properly
19 calibrated over a representative set of 35 rainfall events, considering either infiltration-
20 excess and/or saturation-excess runoff. It was also able to reproduce the measured
21 runoff volume for most of the monitoring period. However, the three years with most
22 rainfall were adequately modelled only including saturation-excess runoff. An analysis
23 performed at the seasonal scale revealed that saturation was modelled in the catchment

24 during almost all of the modelling period, suggesting the importance of this often
25 overlooked process in current modelling attempts.

26 **Keywords: European Loess Belt, Soil erosion, Saturation-excess runoff, WaterSed**
27 **model**

28

Journal Pre-proof

29 **Highlights:**

- 30 - A runoff and soil erosion model was developed: the WaterSed model
- 31 - Its robustness and relative simplicity allowed simulating more than 780 rainfall
- 32 events on an intensively cultivated – while reducing equifinality issues
- 33 - The model simultaneously simulate saturation-excess and infiltration-excess
- 34 runoff
- 35 - Both runoff process should be considered when modelling soil erosion in the
- 36 European loess belt
- 37 - The often overlooked importance of saturation-excess runoff is suggested at both
- 38 the annual and seasonal scale
- 39 - Consequently, runoff and soil erosion models should run continuously
- 40 throughout the hydrological year

41

42 **1. Introduction**

43 Managing soil degradation on arable lands is a major challenge worldwide. In Europe,
44 most rural catchments have undergone strong modifications to facilitate the
45 intensification of agriculture (Robinson and Sutherland, 2002) resulting in numerous
46 on-site and off-site impacts (Stoate et al., 2001; Tarolli and Sofia, 2015). On-site, soil
47 erosion may result in the loss of topsoil, decreasing soil productivity (Durán Zuazo and
48 Rodríguez Pleguezuelo, 2008). Off-site, accelerated soil erosion often results in the
49 degradation of downstream waterbodies and the propagation of muddy flows
50 (Ballantine et al., 2009; Collins and Walling, 2007; Kronvang et al., 2003; Shields et al.,
51 2010; Walling et al., 2003).

52 Regions of intensive agricultural production on the European loess belt have been
53 particularly affected by on-site and off-sites impacts of soil erosion. In central Belgium,
54 off-site soil erosion is estimated to cost between 25 to 75 million euros per year,
55 corresponding to 40 to 120 euros for each ha of arable land (Patault et al., 2021; Van
56 Oost et al., 2002). Several research efforts have therefore been devoted to analyze and
57 quantify the temporal variability and the spatial extent of the areas the most affected.
58 The results pointed out strong spatial and temporal heterogeneities according to the
59 variation of climate forcing and/or the land use evolution as well as the importance of
60 scale effect when moving from the plot to the catchment scale (Cerdan et al., 2004,
61 Delmas et al., 2012). Therefore, knowledge of the spatial variability in sediment
62 production and the identification of the main sediment pathways within the landscape
63 are important.

64 To this end, different types of erosion models have been developed to improve our
65 understanding of sediment dynamics (Aksoy and Kavvas, 2005; De Vente and Poesen,
66 2005; Merritt et al., 2003). These models differ in terms of their complexity, their inputs

67 requirements, the processes they represent, the manner in which these processes are
68 implemented, the scale of application and the types of output information they provide
69 (e.g. Merritt et al., 2003). Fully distributed physically-based models can accurately
70 describe runoff and erosion processes although calibration and model application
71 require significant parametrization. Conversely, empirical models, such as the RUSLE
72 (Revised Universal Soil Loss Equation) (Renard et al., 1997), are frequently used in
73 preference to more complex models because of limited data and parameters
74 requirements, though their ability to comprehensively represent processes at the
75 catchment scale has been questioned (Borrelli et al., 2021; Verstraeten et al., 2007).
76 Expert-based models, such as the Sealing and Transfer by Runoff and Erosion related to
77 Agricultural Management (STREAM) model (Cerdan et al., 2001; Souchere et al., 1998)
78 provide a compromise focusing on the dominant factors driving runoff and erosion in
79 order to avoid over-parameterization and the associated uncertainties.

80 On cultivated areas on the European loess belt, soil surface crusting, surface
81 roughness, total cover (e.g. crops, residues) and antecedent moisture content have been
82 identified as the main determinants of infiltration rates, runoff generation and erosion at
83 the field scale (Chaplot and Le Bissonnais, 2000; Le Bissonnais et al., 2005, 1995). In
84 particular, in the western Paris Basin, France, decision rules were derived by expert
85 judgment based on databases of field measurements to convert soil surface
86 characteristics into soil-related input variables (e.g. infiltration rate, imbibition and soil
87 erodibility (Grangeon et al., 2022). Through incorporating expert-based decision rules,
88 the STREAM model is an effective model which provides runoff and erosion predictions
89 in regions where hortonian overland flow dominates (Cerdan et al., 2002b, 2001; Evrard
90 et al., 2009; Cantreul et al., 2019). Although effective at the field and small catchment
91 scale (Cerdan et al., 2002b, Cerdan et al., 2004), the surface runoff and erosion response

92 from the small catchment (10 km²) to the large catchment (100 – 1000 km²) is still
93 poorly characterized for the Western Paris Basin.

94 Extensive multi-scale field surveys have provided crucial information on the nature
95 and the cause of the scale dependency generally observed for runoff and erosion
96 (Parsons et al., 2006; Wilcox et al., 2003; Yair and Raz-Yassif, 2004). Surface runoff and
97 erosion rates are commonly reported to dramatically decrease with the spatial scale,
98 because of the non-linearity of runoff and erosion processes (Gomi et al., 2008; Moreno-
99 de las Heras et al., 2010; Wainwright, 2002). In temperate cultivated environments of
100 the Northwestern European loess belt, observed variations in runoff coefficients can
101 range from 30–50% for experimental plots to less than 1% for river basins (Delmas et
102 al., 2012; Le Bissonnais et al., 1998). Re-infiltration was identified as a major processes
103 driving this scale dependency on hillslopes and when incorporating this process into the
104 STREAM model, Cerdan et al., (2004) reproduced a decreasing trend for the observed
105 runoff coefficient from the plot scale (500 m²) to the small catchment scale (11 km²).

106 The decreasing trend of runoff coefficients and erosion rates should be modelled
107 according the location of the sources of runoff and sediment and their connection to the
108 flow network (Cammeraat, 2004; Cerdan et al., 2004). Therefore, the relative position,
109 the extent, and the connectivity between areas producing surface runoff/erosion and the
110 infiltrating/deposition areas, link field and small catchment scales (Cerdan et al., 2004;
111 Gumiere et al., 2011).

112 There is therefore a long history of runoff and soil erosion research in the European
113 loess belt since several decades from the plot to the small catchment scale (1m² to 1-
114 10km²) in Belgium, The Netherlands, England, Germany or Poland. Much less studies
115 have investigated the disparity between erosion rates measured at small spatial scales
116 with rates of denudation at larger spatial scales (e.g. river basins with a premanent

117 hydologic network). For empirical models, scaling up erosion rates is achieved with a
118 simple approach to simulate the decreasing trend by applying spatially distributed or
119 regionalized runoff or sediment delivery ratios (Fernandez et al., 2003; Fu et al., 2006;
120 Vigiak et al., 2012). There remains considerable uncertainty regarding the ability of this
121 approach to accurately simulate the spatial variability of water and soil redistribution
122 dynamics.

123 In process-based models, sediment deposition is simulated according to topographic
124 and vegetation cover thresholds (mainly slope and roughness) that affect the flow
125 velocity. For example, in the STREAM model, for each threshold, a suspended sediment
126 concentration for the transport capacity was defined based on experimental studies and
127 fields surveys (Cerdan et al., 2002a, 2002b). Values of these thresholds are therefore
128 adapted to scales ranging from the hillslope to the headwater catchment scale. Indeed
129 most of the models that have been developed or applied in the context of the European
130 loess belt are based on concepts that are most suited to reproduced hillslope
131 geomorphology processes. They consider that the soil surface is the limiting factor in
132 terms of infiltration (mostly hortonian runoff, with or without taking into account soil
133 crusting processes). At the hillslope scale, and for a single event this hypothesis is
134 acceptable. However, there is a need to tests these concepts on larger temporal (several
135 decades) and spatial scales (more than 100 km²).

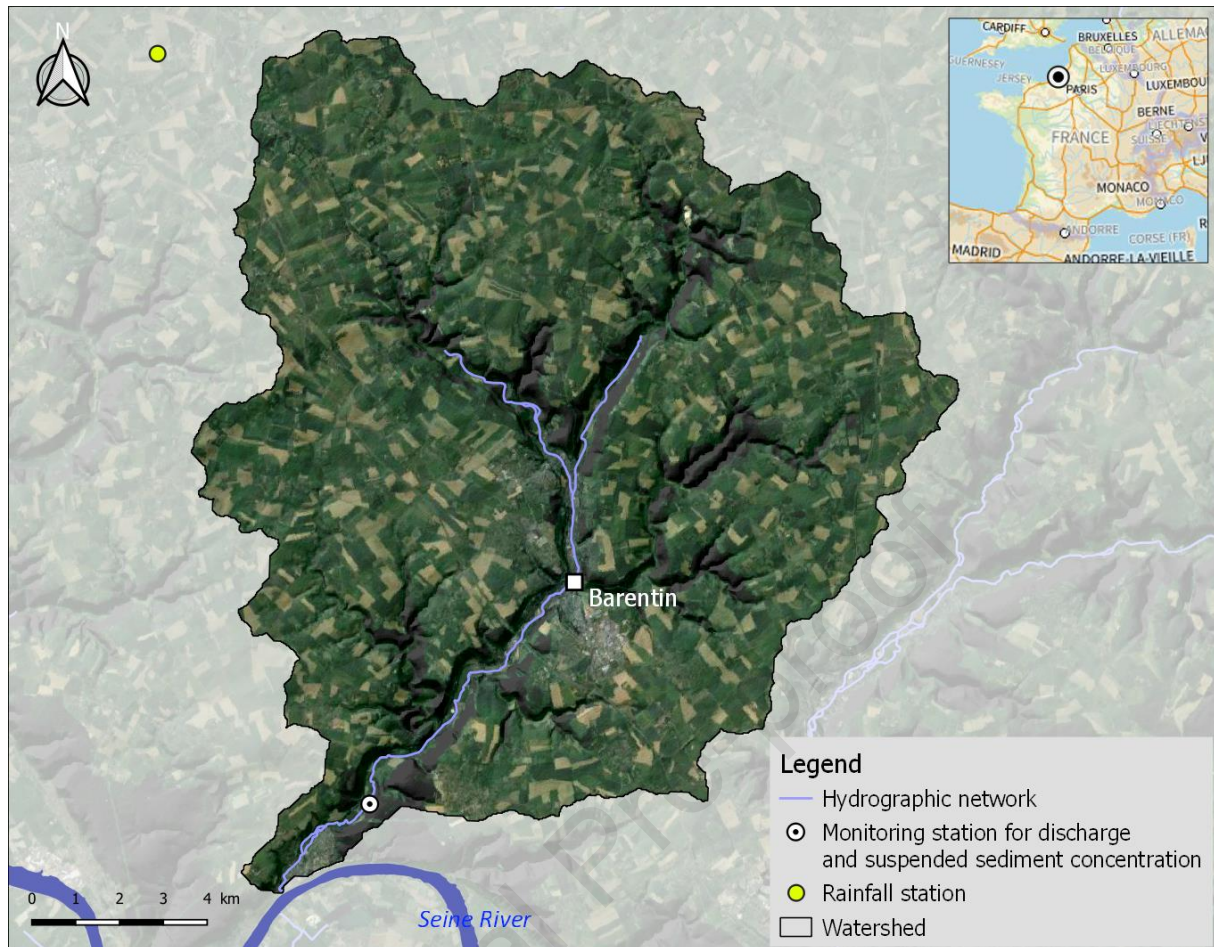
136 However, a limited number of erosion numerical models can account for both
137 saturation-excess and infiltration-excess runoff, limiting their ability to represent
138 catchments dynamics under various intra- and inter-annual rainfall depth variations. In
139 this study, we therefore describe a new runoff and erosion model: the WaterSed (Water
140 and Sediment). Based on the STREAM (Cerdan et al., 2001) and LISEM (De Roo et al.,
141 1996) concepts, We develop a process-based model that focus on the dominant

142 processes. Its main novelty are to be able to allow simulations of large catchment over
143 several years (to reflect the diversity of initial conditions in terms soil surface conditions
144 and soil saturation) while avoiding too many equifinality issues and that it permits to
145 test the relative importance of both saturation-excess and infiltration-excess runoff at
146 the catchment scale. The model was tested using an extensive dataset including 12 years
147 (September 1998- August 2011) of measured rainfall, discharge, suspended sediment
148 concentration as well as land use scenario, collected in Upper Normandy, France. The
149 combined effects of both crusting on agricultural fields and large temporal rainfall
150 variability were studied, and their consequences on runoff and erosion modelling were
151 highlighted. More specifically, we tested the hypothesis that saturation-excess may be a
152 relevant process to consider in modelling approaches even on soils that may be affected
153 by surface crusting, and tried to quantify its importance.

154 **2. Material and methods**

155 **2.1. Study site**

156 The Austreberthe catchment (214 km²) is located in Upper Normandy, France
157 (Figure1).



158

159 Figure 1: Location of the Austreberthe basin in Upper Normandy.

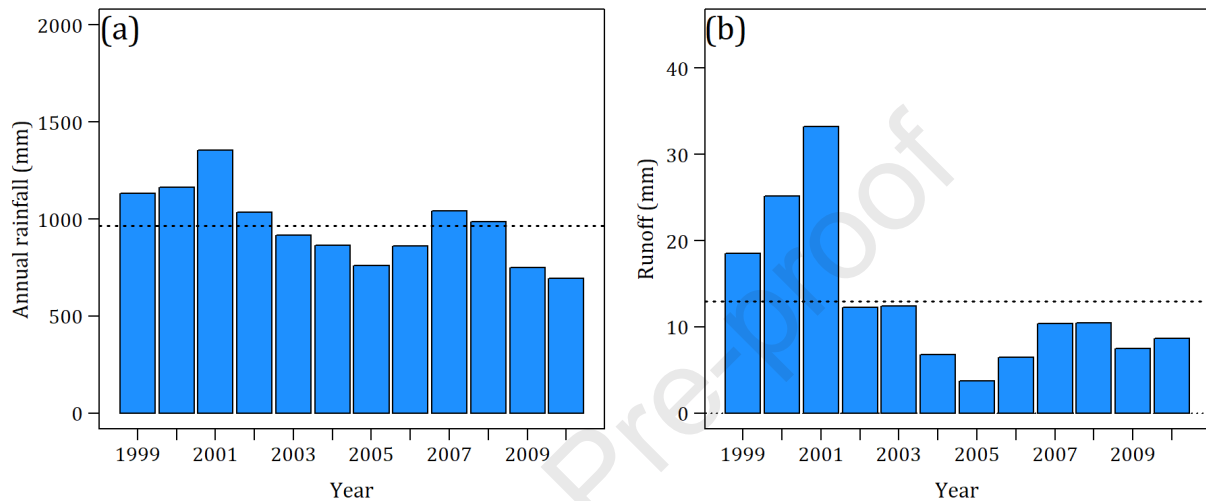
160

161 The region is characterized by loess plateaus of moderate elevation (<300 m) mainly
 162 covered by crops (53.7%), pastures (29.7%), forests (9.5%) and urban areas (5.8 %),
 163 and incised valleys exhibiting steep slopes (mean 5%, maximum 30%), mainly covered
 164 by forests and grasslands. The geology is composed of a sedimentary substratum, mainly
 165 Upper Cretaceous chinks, covered by clay-with-flints, Tertiary sandy-clay residual
 166 deposits and loess (Hauchard and Laignel, 2008; Laignel et al., 1999; Quesnel et al.,
 167 1996). The region's climate is moderate oceanic with annual average temperature of
 168 approximately 13°C (Delmas et al., 2012).

169 The catchment hydrology over the study period was characterized by relatively wet

170 years during the 1999-2001 period (rainfall depth was 26% above the mean of 964 mm)

171 and dry years during the 2003-2006 and 2009-2010 periods (rainfall depth was 12%
 172 and 25% below the mean, respectively) (Figure 2). Consequently, runoff was low during
 173 2003-2006 and 2009-2010. Of note, the runoff was very high during the 1999-2001 wet
 174 period; runoff was 97% above the mean, continuously increasing over the course of this
 175 period.



176

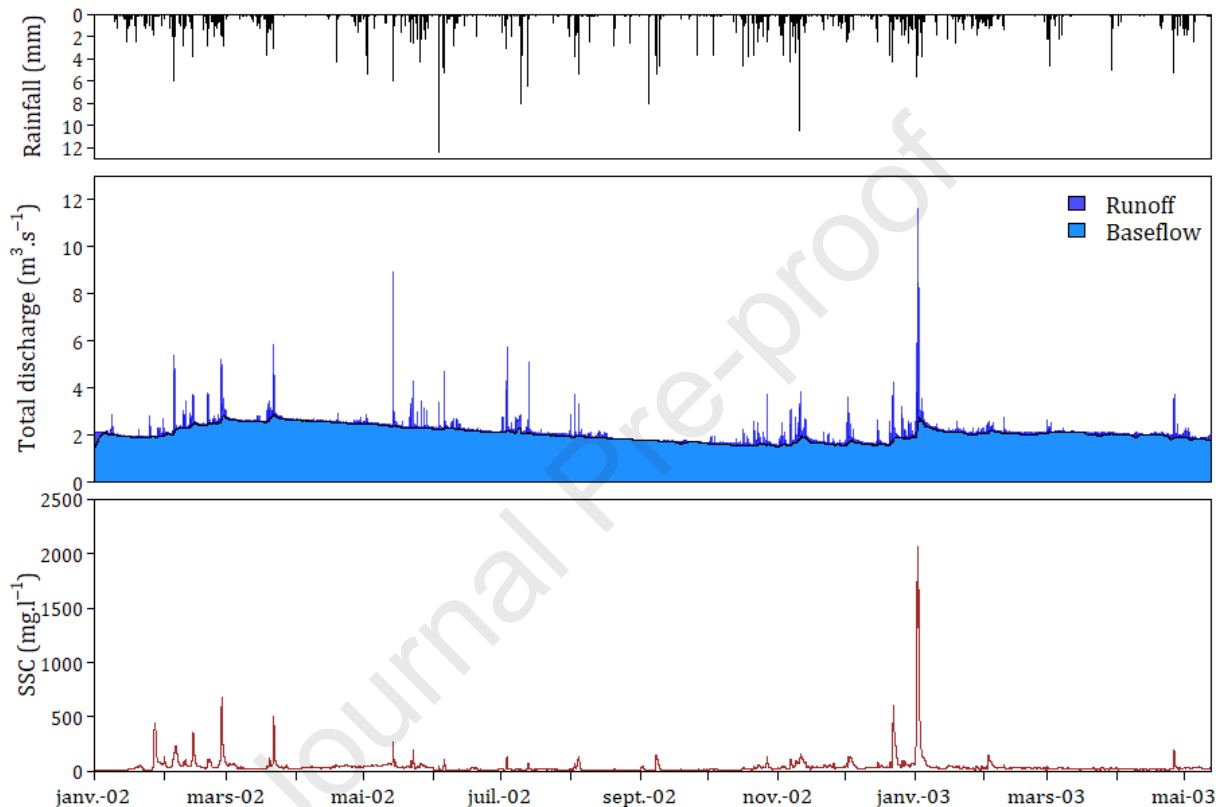
177 Figure 2: Annual (a) rainfall and (b) runoff measured between 1999 and 2010. The
 178 dotted line in subfigure (a) is corresponding to the annual mean, calculated over 12
 179 years.

180

181 **2.2. Discharge and suspended sediment concentration measurements and** 182 **analysis**

183 Two different data sets were used in this study (Figure 3). First, high frequency
 184 discharge and Suspended Sediment Concentration (SSC) measurements were acquired
 185 in previous research on the Austreberthe River (Laignel et al., 2006, 2008).
 186 Measurements were performed at 30-min time steps between January 2002 and May
 187 2003. Rainfall time series was acquired from using a gauge station at 0.2 mm resolution.
 188 Then, a daily discharge time series was acquired over the period September 1998 –

189 August 2010. Rainfall over this period was extracted from the SAFRAN database
190 (Durand et al., 1993).
191 Runoff was estimated from the discharge time series using the methodology proposed
192 by Lyne and Hollick (1979) . In the following, only runoff will be considered.
193



194
195 Figure 3: Rainfall, discharge and suspended sediment concentration high frequency time
196 series (from top to bottom) used for calibration.

197

198 Rainfall events were defined as events with rainfall depth higher than 2 mm, and
199 separated from another event by 24h without rainfall. Flood events were defined
200 manually for 30 min time series by identifying the beginning of the rising limb and the
201 end of the falling limb. For daily time series, we assumed that the daily runoff volume

202 was generated by the corresponding daily rainfall. In total, 35 coupled rainfall-runoff
203 events were extracted for 30 min time series and 782 events for daily time series.
204 For each of these coupled events, the following variables were calculated: rainfall depth
205 (mm), rainfall duration (minutes), rainfall depth over the previous 48 hours (mm),
206 maximum rainfall intensity ($\text{mm}\cdot\text{h}^{-1}$), runoff volume (m^3), runoff duration (h), runoff
207 peak ($\text{m}^3\cdot\text{s}^{-1}$), and suspended sediment load (t).

208

209 **2.3. Catchment characteristics and model preprocessing**

210 **2.3.1. DEM and stream network**

211 The Digital Elevation Model (DEM) was extracted from BD Alti®, providing elevation
212 at a 25 m spatial resolution. Depressions were filled according the algorithm developed
213 by Wang and Liu, (2006). The stream network location and width were extracted from
214 BD Carthage 2013® and used for stream burning.

215 **2.3.2. Land use and soil surface characteristics**

216 Land use was divided into 9 classes: winter crops, early spring crops, late spring
217 crops, permanent crops, bare soils, grasslands, forests, urban areas, water surface. Given
218 that crops vary from one year to another, annual land use map for each of the 12 studied
219 years (1998-2010) were create using three national datasets. The French Land Parcel
220 Identification System (RPG), Corine Land Cover and the General Census of French
221 Agriculture (RGA) provided detailed plot delineation and observed land use for the
222 2006-2012 period over the whole catchment.

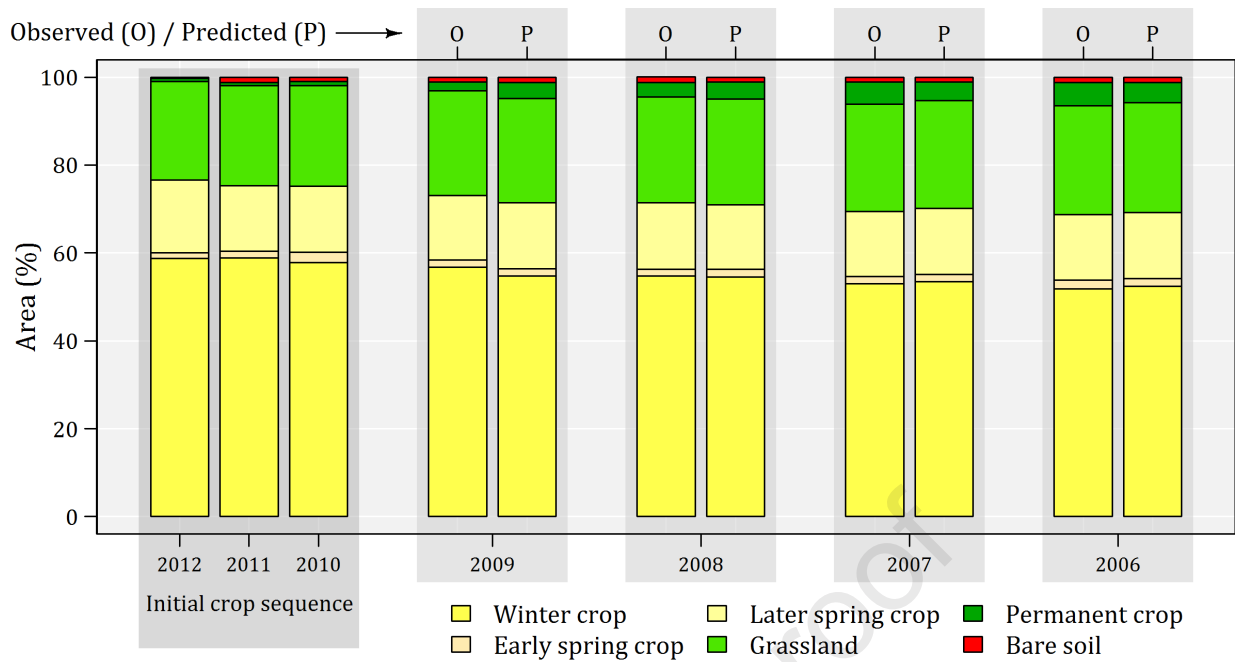
223 Then, the land use for the 1998-2005 period was extrapolated by applying statistical
224 crop sequence rules developed on the 2006 and 2012 period. Based on 3-years crop
225 sequences (usual in this part of France) on the recorded 2006-2012 period, probabilities
226 of antecedent crop were determined (Table 1) and applied from 2012 to 1998.

Three-year crop sequence	Crop type probabilities (%)					
	W	ES	LS	G	PC	BS
W+W+W	77.4	2.7	14.5	1.0	3.3	1.0
W+W+ES	93.1	1.7	3.4	0.8	0.7	0.2
W+W+LS	84.6	1.9	8.7	2.2	0.8	1.7
W+W+G	47.7	0.8	4.7	44.9	1.6	0.3
W+W+PC	85.5	3.7	1.0	0.5	9.1	0.1
W+W+BS	91.9	1.6	2.3	0.5	0.6	3.1

228 Table 1: Example of crop probabilities before for the three-year crop sequence
 229 beginning with winter crop. W: Winter crop; ES: Early spring crop; LS: Late spring crop;
 230 G: Grassland; PC: Permanent crop; BS: Bare soil.

231

232 The 2012-2006 period was used to evaluate if the reconstruction procedure matched
 233 the observed crops (Figure 4). Crops were then simulated from 2005 to 1998, resulting
 234 in 12 land use maps with 9 land use classes, over the 1998-2010 period.



235

236 Figure 4: Simulation of crops between 2009 and 2006 according crop sequence rules
 237 and backward propagation. Simulated crops (P) are compared to the observed crops (O)
 238 at the Seine-Maritime department level.

239

240 Based on numerous previous studies performed in this region, it is assumed that soil
 241 surface crusting, surface roughness, cover and texture mainly control the soil
 242 hydrological and erosion behavior at the field scale. Monthly crusting, roughness and
 243 cover were therefore defined for each crop type, based on the previously developed land
 244 use maps, according to Evrard et al., (2010), modified in order to integrate intercrops
 245 after harvesting in October and November. The soil texture map was derived from the
 246 superficial formations map of the French Geological Survey with a precision of 1:50 000
 247 into three classes: sand, silt, clay.

248

249

250

251 **2.4. Model inputs**

252 Finally, the land use-texture combination was used to calculate the monthly model
253 inputs for 27 possible combinations (9 land uses x 3 textures) over 12 years:

- 254 • Steady-state infiltration and potential sediment concentration were assigned to
255 each soil surface characteristics according to Cerdan et al., (2001) and Cerdan et
256 al., (2002b).
- 257 • Manning's values were derived from surface roughness (Morgan, 2005) and the
258 crop cover (Gilley et al., 1991).
- 259 • The soil erodibility factor was adapted from Souchère et al., (2003a).

260 The corresponding calculations were detailed in the paper and toolbox presented in
261 Grangeon et al. (2022). In short, default values were assigned to each soil surface
262 characteristics (i.e. crop cover, crusting stage, roughness) combination, and were
263 adjusted depending on the soil texture, over time at a monthly scale to reflect the effect
264 of rainfall on vegetation cover, surface sealing and roughness, but also to reflect the
265 possible crop operations effects on soil surface (e.g. harvesting and ploughing increasing
266 infiltration capacity through decreased vegetation cover and surface sealing). The
267 Manning's coefficient considered only soil roughness and crop cover.

268 For each of the 782 coupled rainfall-flood events, the following inputs were calculated:

- 269 • Rainfall depth and duration

270 **2.5. Rainfall imbibition (mm) was deduced according to the table developed by**
271 **Cerdan et al., (2001) using the infiltration capacity and the 48h antecedent**
272 **rainfall depth. The WaterSed model**

273 The WaterSed model is a raster-based, event-scale runoff and erosion model.

274 **2.5.1. Water module**

275 **Water balance – Runoff generation**

276 For each simulated rainfall event, an hydrologic balance HB_i (mm) is calculated
 277 (Cerdan et al., 2001) as:

$$HB_i = R_i - IR_i - (IC_i \cdot t_{eff_i})$$

$$\text{If } HB_i > 0 \text{ then } HB_i = E_{R_i} \cdot \theta \quad (1)$$

$$\text{If } HB_i < 0 \text{ then } HB_i = \Delta I_i$$

278 Where R_i is the rainfall depth (mm), IR_i the imbibition rainfall (mm), IC_i the
 279 steady-state infiltration rate ($\text{mm} \cdot \text{h}^{-1}$), and t_{eff_i} the effective rainfall duration (min) of
 280 the i th cell. Positive values indicate an excess rainfall (E_{R_i} , mm), while negative values
 281 indicate potential infiltration for upstream runoff (ΔI_i , mm). Excess rainfall E_{R_i} can be
 282 modified with an adjustment parameter (θ), varying from 0 to 1, in order to considering
 283 scale effect from grid resolution.

284 Saturation processes were introduced by limiting the infiltration by a maximum
 285 water storage WS_i (mm):

$$HB_i = R_i - WS_i \quad \text{if} \quad IR_i + (IC_i \cdot t_{eff_i}) > WS_i \quad (2)$$

286 **Flow velocity and flow travel time – preprocessing water**

287 Eq. 1 is assumed reasonable for small catchments (in the order 100 ha), when the
 288 flow travel time to the outlet is within the same order of magnitude of the effective
 289 rainfall duration. For larger catchments, where flow travel times may be longer, Eq. 1
 290 may result in an underestimation of re-infiltration processes. Accordingly, the WaterSed
 291 model estimates the continuous abstraction for the runoff duration for each cell with the
 292 calculation of runoff duration requiring an estimation of the velocity and the flow travel
 293 time for each cell.

294 Average excess rainfall intensity, e_i (mm.h^{-1}), is derived from excess rainfall, E_{R_i} (mm),
 295 as:

$$e_i = E_{R_i}/t_{eff_i} \quad (3)$$

296 Overland flow travel time in a cell is estimated with Manning's formula (Chow, 1988;
 297 Melesse and Graham, 2004) with overland flow velocity, V_{H_i} (m.s^{-1}) calculated as:

$$V_{H_i} = (S_i^{0.3} L_i^{0.4} e_i^{0.4})/n_i^{0.6} \quad (4)$$

299 where S_i is the slope of surface in cell i (m.m^{-1}), L_i is the flow length of the cell, (i.e.
 300 equal to cell size or north-south and east-west flow), and equal to $\sqrt{2}$ times cell size for
 301 diagonal flow directions, and n_i is the Manning's roughness coefficient ($\text{s.m}^{-1/3}$).

302 Channel flow velocity, V_{C_i} (m.s^{-1}), is estimated by combining Manning's equation and
 303 the steady state continuity equation for a wide channel (Chow, 1988; Muzik, 1996):

$$V_{C_i} = S_i^{0.3} \left(\frac{Q_i}{W_i} \right)^{0.4} n_i^{-0.6} \quad (5)$$

304 where Q_i is the cumulative discharge through the cell, obtained by summing upstream
 305 flow contributions and the contribution from precipitation excess for that cell i
 306 ($\text{m}^3.\text{s}^{-1}$), and W_i is the channel width (m). To avoid unrealistic velocities values for
 307 hillslopes and channels, a minimum velocity of 0.02 m.s^{-1} and a maximum velocity of 2
 308 m.s^{-1} are applied based on the common range incorporated into hydrologic models
 309 (Grimaldi et al., 2010). The travel time for each cell is calculated by dividing travel
 310 distance by cell velocity.

311 The flow through a given cell during the runoff duration can be described with a
 312 runoff hydrograph. Here, a triangular unit hydrograph was chosen and accordingly, the
 313 time of concentration T_{C_i} (min) (i.e. the time required for runoff to travel from the
 314 hydraulically most distant point in the watershed to the outlet) is calculated for each cell

315 by summing up upslope travel time. Runoff is assumed to begin at the centroid of the
 316 effective rainfall ($t_{eff_i}/2$). Therefore, the runoff duration T_{R_i} (min) is calculates as:

$$T_{R_i} = \left(\frac{t_{eff_i}}{2} + T_{C_i} \right) \cdot \alpha \quad (6)$$

317 This recession parameter α was introduced to adjust re-infiltration and to take into
 318 account potential errors on the flow travel time estimations (e.g. Grimaldi et al., 2012).
 319 Therefore, re-infiltration is re-evaluated based on the runoff duration minus rainfall
 320 duration for each cell.

321

322 ***Water routing - Runoff volume transfer***

323 Once the calculation of the water balance, flow velocity and travel time is calculated,
 324 the water volume is routed according the Single Flow Direction (SFD) algorithm, in
 325 which the flow is concentrated in a single width cell.

326 Previously calculated water volumes are accumulated at the catchment scale from the
 327 runoff / infiltration balance calculated for each cell incorporating runoff flow network. A
 328 two-step calculation allows cells to re-infiltrate the totality or a part of generated
 329 upstream surface runoff. Accordingly, the hydrological balance is calculated once at the
 330 beginning of the simulation and a second time during the flow routing.

331 Using the total runoff volume through a cell, V_i (m^3), the runoff duration, and
 332 assuming a triangular unit hydrograph for each cell, a runoff peak, Q_{peak_i} ($m^3.s^{-1}$), is
 333 computed as:

$$Q_{peak_i} = 2V_i/T_{R_i} \quad (7)$$

334 2.5.2. Sediment module

335 ***Sheet and gully erosion - sediment generation***

336 The model assumes that topography, soil surface characteristics, and rainfall
 337 characteristics are the main determinants for interrill and concentrated erosion (Cerdan
 338 et al., 2002c; Martin, 1999). For interrill erosion, a table is used to assign a potential
 339 sediment concentration in the flow, SC_i (g.l^{-1}), to each combination of soil surface
 340 characteristics and rainfall intensity (Cerdan et al., 2002b). The corresponding interrill
 341 erosion, IE_i (kg), is calculated as:

$$IE_i = E_{R_i} \cdot SC_i \quad (8)$$

342 where E_{R_i} , (m^3), is the excess rainfall. Gully erosion occurs when the peak discharge on a
 343 hillslope grid cell exceeds a threshold peak discharge, Q_{crit} ($\text{m}^3 \cdot \text{s}^{-1}$), defined as a model
 344 parameter. The threshold peak discharge can be estimated by comparing the location of
 345 gullies on aerial photography and those predicted by the model.

346 A gully is assumed to be rectangular and unique per cell. The calculation of the cross
 347 section requires first the gully width, W_{G_i} (m), calculated from an empirical relationship
 348 developed by Nachtergaele et al., (2002) as:

$$W_{G_i} = 2.51 Q_{peak_i}^{0.412} \quad (9)$$

349 Next, flow velocity, V_{G_i} ($\text{m} \cdot \text{s}^{-1}$) is computed according to the empirical relationship
 350 developed by Govers, (1992) as:

$$V_{G_i} = 3.52 Q_{peak_i}^{0.294} \quad (10)$$

351 Then gully height, H_{G_i} (m), is deduced from the gully width W_{G_i} , the gully velocity V_{G_i} ,
 352 and the peak discharge Q_{peak_i} , as:

$$H_{G_i} = Q_{peak_i} / (W_{G_i} V_{G_i}) \quad (11)$$

353 The gully cross section, A_{G_i} (m^2) is finally determined from the gully width W_{G_i} and
 354 the gully height H_{G_i} (Eq. 12). A maximum cross section value of 0.25 m^2 is fixed in order
 355 to avoid unrealistic values. The gully volume VOL_{H_i} (m^3) is then obtained by multiplying

356 this cross section of incision by the grid cell length (Eq. 13). The gully volume is
 357 weighted by a soil erodibility factor, EF_i (-), in the range [0-1] computed from rules
 358 adapted from the methodology developed by Souchère et al., (2003a) to determine the
 359 sensitivity to gully erosion.

$$A_{G_i} = W_{G_i} \cdot H_{G_i} \quad (12)$$

$$VOL_{H_i} = A_{G_i} \cdot L_i \cdot EF_i \quad (13)$$

360 Last, the gully erosion, GE_i (kg) is calculated by multiplying the gully volume VOL_{G_i} by
 361 the bulk density, ρ (kg.m⁻³), as:

$$GE_i = VOL_{G_i} \cdot \rho \quad (14)$$

362 Therefore, the total gross erosion, TE_i (kg), of a cell corresponds to the sum of the
 363 interrill erosion and gully erosion as:

$$TE_i = IE_i + GE_i \quad (15)$$

364 ***Sediment mass transfer – sediment yield and deposition***

365 At the catchment scale, sediment is transported in proportion to the runoff volumes.
 366 For cell i producing runoff, the mass of sediment transported downstream, SY_i (kg), is
 367 expressed as:

$$SY_i = SY_\alpha + TE_i \quad (16)$$

368 Where SY_α is the mass of sediment coming from upslope cells (kg), and TE_i is the total
 369 gross erosion (kg). The sediment mass is transported along with runoff, using the single
 370 flow direction algorithm.

371 Sediment deposition occurs in two cases. First, if a cell has the potential to infiltrate a
 372 part or the totality of the upslope runoff, the mass of deposited sediment, SD_i (kg) (Eq.
 373 17), corresponds to the product of the infiltrated water volume, ΔI_i (m³), and the mean
 374 suspended sediment concentration of the flow, \overline{SC}_i (g.l⁻¹) (Eq. 18).

$$SD_i = \Delta I_i \cdot \overline{SC}_i \quad (17)$$

$$\overline{SC}_i = SY_\alpha / V_\alpha \quad (18)$$

375 Where V_α is the runoff coming from upslope cells (m^3). In this case, the sediment yield
376 becomes:

$$SY_i = SY_\alpha - SD_i \quad (19)$$

377 Second, sediment deposition occurs when the mean suspended sediment concentration
378 of the flow \overline{SC}_i exceeds the suspended sediment concentration for the sediment
379 transport capacity, SC_{TC_i} ($g.l^{-1}$). In this case, the sediment yield is calculated as:

$$SY_i = V_i \cdot SC_{TC_i} \quad (20)$$

380 Where V_i (m^3) is the runoff volume leaving the cell i . The mass of deposited sediment is
381 then deduced as:

$$SD_i = SY_\alpha - SY_i \quad (21)$$

382 The suspended sediment concentration for the transport capacity, SC_{TC_i} is calculated
383 as the ratio between the slope S_i and the Manning's roughness coefficient n_i (Eq. 21).

$$SC_{TC_i} = \overline{SC}_i \cdot \exp\left(-\beta \cdot \frac{n_i}{h_{peak_i}}\right)$$

384 Where β is a sediment settling parameter (-) and h_{peak_i} is the corresponding water
385 height to the peak discharge Q_{peak_i} . In this case, sediment deposition is expressed as:

$$SD_i = (\overline{SC}_i - SC_{TC_i}) \cdot V_i \quad (23)$$

387

388 2.6. Model calibration and application

389 For simulating runoff and erosion at the catchment scale, 4 parameters need
390 calibration: the scale effect parameter θ , the recession coefficient α , the threshold
391 discharge for gully initiation Q_{crit} and the sediment settling parameter β . Of note, this
392 number of parameter is relatively small relative to runoff and erosion models applied to

393 the catchment scale. The model was calibrated against 35 coupled rainfall-flood events
 394 using the high-frequency measurements available over the 2002-2003 period. The Nash-
 395 Sutcliffe efficiency (NSE) and the Root Mean Square Error (RMSE) were used for
 396 quantitative evaluation of the model performances:

$$NSE = 1 - \frac{\sum_{i=1}^n (V_{pred} - V_{obs})^2}{\sum_{i=1}^n (V_{pred} - \overline{V_{obs}})^2} \quad (24)$$

$$RMSE = \sqrt{(1/n) \sum_{i=1}^n (V_{pred} - V_{obs})^2} \quad (25)$$

397 where V_{obs} is the observed value (runoff volume or sediment mass) for the considered
 398 rainfall/runoff event, V_{pred} is the predicted value, $\overline{V_{obs}}$ is the mean of the observed
 399 values, and n the number of rainfall/runoff events. Calibrated parameter values were
 400 used for modelling over the September 1998-August 2010 period.

401 In order to analyze the respective effects of infiltration-excess and saturation-excess
 402 runoff, the model was calibrated using two different configurations: i) considering only
 403 infiltration-excess runoff (saturation-excess runoff was not allowed to occur) and ii)
 404 considering both infiltration-excess and saturation-excess runoff.

405 In this study, the water storage was spatially distributed using the pedology as input
 406 data: Because no specific measurements were available, we arbitrarily attributed an 80
 407 mm and 150 mm storage value to the 2 main pedological entities of the catchment,
 408 namely flint clays and deep loam soils, respectively. The model was run using a “quasi-
 409 continuous” approach: the spatially-distributed water content at the end of a run was
 410 used as input value for the following event, applying drainage in-between the modelled
 411 events. This approach was previously successfully applied (Grangeon et al., 2021) to
 412 model the runoff and erosion dynamics of an alpine catchment. In the current study, as

413 the modelling period was long (> 10 years) and due to a lack of data, for simplicity
 414 reasons, the water storage drainage value was set as a constant value of 4 mm.d⁻¹,
 415 following a simple trial-and-error approach.

416 3. Results and discussions

417 Between 2002 and 2004, 35 rainfall-runoff events were extracted from time series of
 418 rainfall, discharge and SSC for the model calibration (Table 2). Rainfall amounts ranged
 419 from 3.6 mm to 58.7 mm with varying conditions of antecedent rainfall depth (from 0.2
 420 mm to 35.2 mm) and maximum intensity at 6 min (from 2.0 mm.h⁻¹ to 12.8 mm.h⁻¹).
 421 Runoff volumes ranged from 2,171 m³ to 671,350 m³, with runoff coefficients ranging
 422 from 0.21% to 5.34%.

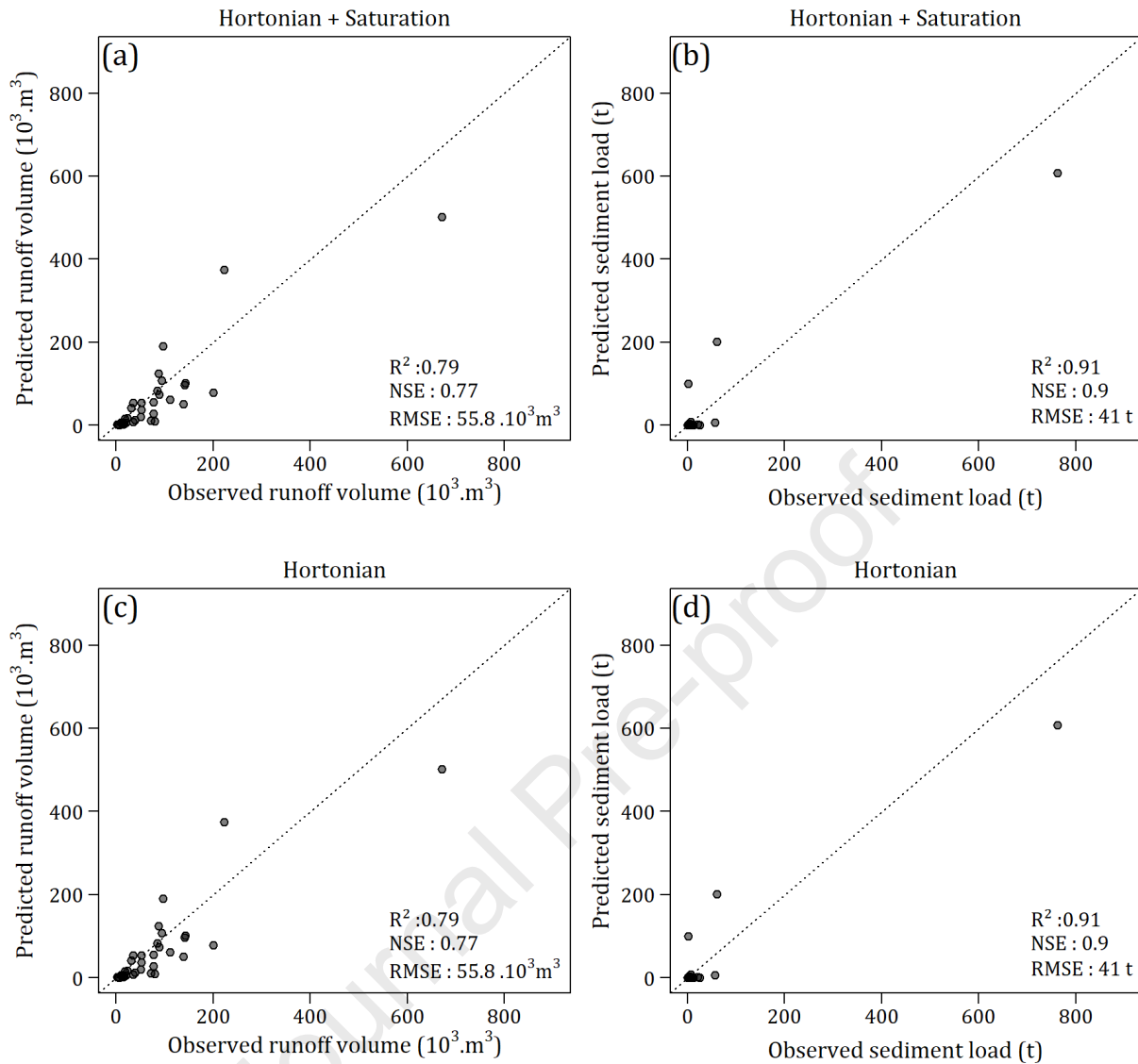
423

	Min.	Median	Max.
N = 35			
Rainfall (mm)	3.6	21.2	58.7
Maximum 6 min intensity (mm/h)	2.0	5.2	12.8
Antecedent 48h rainfall depth (mm)	0.2	1.2	35.2
Runoff (m ³)	2 171	52 462	671 350
Runoff coefficient (%)	0.21%	1.22%	5.34%
Sediment load (t)	0.1	2.9	762.3

424 Table 2: Characteristics of rainfall events used for the WaterSed model calibration

425 The WaterSed model has been calibrated with and without the possibility of soil
 426 surface saturation on these events. The prediction performances on runoff volumes and
 427 sediment fluxes are presented in Figure 5. The parameters optimised by the calibration
 428 are presented in Table 3.

429



430

431

432 Figure 5: Observed versus predicted values of runoff volumes (a) and (c) and sediment
 433 loads (b) and (d) by the WaterSed model after calibration for the Austreberthe River.

434

435 Model prediction quality for runoff volume and sediment load is good with a NSE of
 436 ca. 0.7 for runoff volumes and for sediment loads. Overall results are above the classical
 437 threshold values for satisfactory model, defined between $0.5 < NSE < 0.65$ in
 438 hydrological studies (Moriassi et al., 2007; Ritter et al., 2013).

439

440

Parameter	Hortonian	Hortonian + Saturation
θ – Grid size effect	0.19	0.13
α – Recession	2	2
Q_{crit} – Threshold discharge	0.01	0.01
β – Sediment settling	0.00013	0.00030

441 Table 3: WaterSed calibration parameters

442

443 Calibration results show it is possible to achieve good model accuracy with or without
444 taking into account the saturation of the soil profile. The difference for the runoff
445 calibration lies in the values of the calibration parameter “grid size effect”; 0.19 with
446 “hortonian” only and 0.13 in the case of “hortonian + saturation”. The grid size effect
447 parameter is a calibration parameter that permits to take into account the difference
448 between the spatial resolution at which were collected the observed reference values
449 and the one at which the model is applied. It is especially true for hydraulic conductivity,
450 which tend to decrease with increase slope length (reinfiltration processes). Therefore,
451 if hydraulic conductivity measurements at the scale of few centimeters (typical size of
452 measurement devices) is used it in a model with a cell size of several meters (typical size
453 of hydrological models), a correction is needed for the difference. This parameter is
454 therefore very sensitive, a value of 1 means no reinfiltration is foreseen because of the
455 model cell size (e.g. infiltration parameters measured on a rainfall simulation plot of 25
456 m², and same model cell size), a value of 0.1, means you expect a potential reinfiltration
457 of 90% of your runoff. Here the values are quite similar, meaning that at the rainfall-
458 runoff event scale, we can obtain similar results with or without taking into account
459 saturation processes of the soil profile for the chosen rainfall-runoff events, provided
460 that the model is adequately calibrated. This result underlines that even using a simple

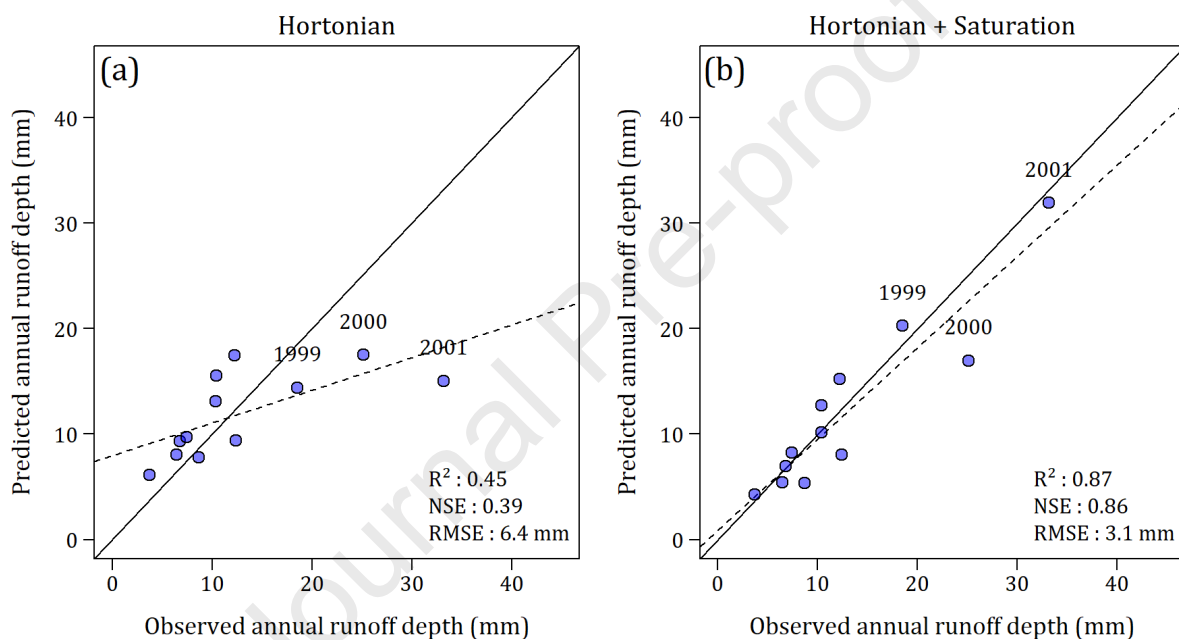
461 model (only four parameters were used to parameterize the runoff and erosion model),
462 equifinality issues (Beven et al., 2001) may arise and that model parameterization
463 should be based on a sound understanding of the catchment behavior. Previous studies
464 on agricultural catchments (e.g. Saffarpour et al., 2016; Grangeon et al., 2021) suggested
465 that both infiltration-excess and saturation-excess may occur in agricultural catchments.
466 Consequently, we used the model to analyze the relative effects of these two processes
467 in a catchment of the European Loess belt, where model considering infiltration-excess
468 only are recurrently being used (Baartman et al., 2020), and tested the hypothesis that
469 saturation-excess may be a relevant process to consider.

470 It is accepted that, in agricultural catchments covered with silty soils, rainfall
471 progressively results in soil surface crusting, dramatically decreasing infiltration rates,
472 and changing runoff-generating mechanism from saturation-excess runoff to infiltration-
473 excess runoff (Boardman, 2020). However, this transition has rarely been quantified
474 over the course of multiple hydrological years, limiting our understanding of runoff
475 occurrence in such catchments.

476 We tested the validity of the calibrated model over a long time period (12 years),
477 between September 01, 1998 and August 31, 2010 (Figure 6). During this period, the
478 mean annual precipitation accumulation is 964 mm with a minimum of 694 mm in 2010
479 and a maximum of 1356 mm in 2001 (Figure 2). The years 1999 to 2002 are particularly
480 wet compared to the following eight years, which were relatively dry, except for 2007
481 and 2008.

482 The runoff interannual variability generally follows the same trend. The years 1999,
483 2000 and 2001 are the years with the highest runoff depths, with 18.5 mm, 25.1 mm and
484 33.1 mm, respectively. For the other nine years, the average annual runoff is 8.7 mm,
485 with a minimum in 2005 of 3.7 mm.

486 During this period, 782 rainfall events greater than 2 mm were recorded, covering a
 487 wide range of rainfall depths and intensity. All of these events were modelled by
 488 applying the previously calibrated parameters.
 489 Predicted runoff volumes per event were aggregated on an annual basis and compared
 490 to observed annual runoff. With the hortonian module alone, the R^2 of 0.45 and the NSE
 491 of 0.39 indicate poor prediction performance. The wettest years (1999, 2000 and 2001)
 492 are underestimated while the driest years are slightly overestimated.

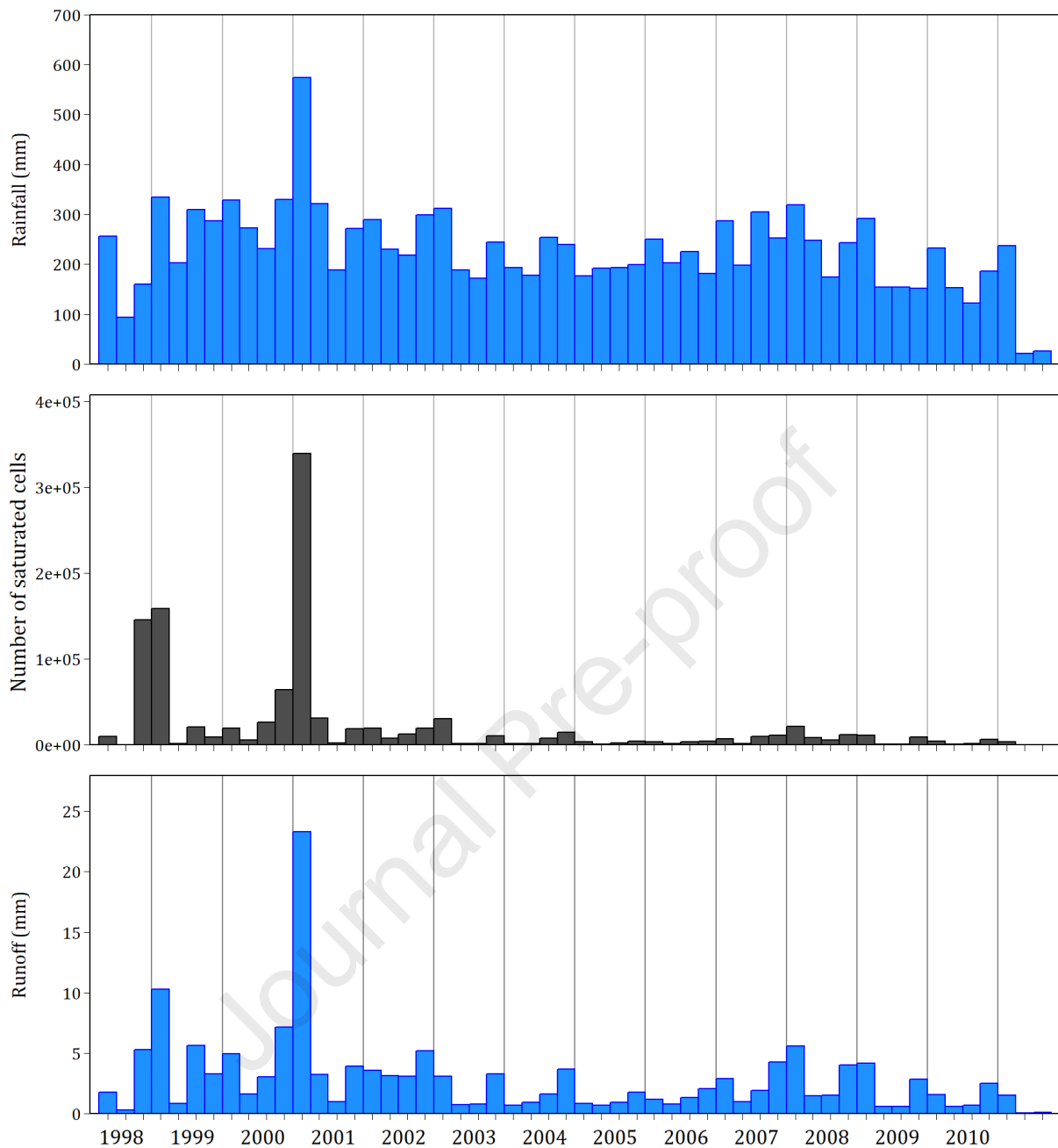


493
 494 Figure 6: Observed versus predicted values of runoff volumes (a) with the hortonian
 495 module (b) with the hortonian + saturation modules by the WaterSed model for the
 496 Austreberthe River between 1998 and 2010.

497
 498 The integration of the possibility to saturate the soil profile permits to increase the
 499 model performance, especially for the 2001 year, which was exceptionally wet. If we
 500 model only the period between 2002 and 2010, both model performances would be very
 501 comparable and the integration of a saturation runoff module would not appear
 502 pertinent. This modelling study therefore underlines that an adequate modelling of the

503 Austreberthe catchment, mostly covered with silty soils, would require the
504 consideration of saturation-excess runoff. However, if we calculate the number of
505 saturated cells at the scale of the catchment (Figure 7) using the soil saturation module,
506 we clearly visualize their importance for the wettest years but we also realize that there
507 are always part of the catchment that exhibit saturated cells even for the dry years. On
508 note, there is a significant number of saturated cells during the calibration years
509 especially in 2002, which can explain the better results obtained with hortonian +
510 saturation modules (Fig. 4). It is therefore suggested that saturation-excess runoff
511 should be considered at the seasonal and probably at the rainfall event scale, although in
512 a smaller proportion, when studying the runoff dynamics of agricultural catchment
513 covered with silty soils.

514



515

516 Figure 7: Rainfall, number of saturated cells and runoff depth calculated at the seasonal
 517 scale between 1998 and 2010 for the Austreberthe catchment.

518

519 The importance of soil saturation on runoff and erosion processes has almost never
 520 been studied in the context of the cultivated soils of the European loess belt. Most of the
 521 research has focused on soil surface conditions, i.e. surface crust development,
 522 roughness and vegetation cover, that have an important influence on infiltration rates,

523 runoff generation and erosion (Papy and Douyer, 1991; Auzet et al., 1995), particularly
524 at the local scale. On bare, cultivated soils, crusting has been used to describe surface-
525 structure evolution, as it has a very strong influence on soil hydraulic properties and
526 runoff rate. Crusting also affects soil surface shear strength and roughness, which
527 influence, together with vegetation cover, sediment detachment and transport processes
528 (Le Bissonnais et al., 2005). Relationships between the different types of surface
529 conditions and quantitative runoff and soil erosion parameters have therefore been
530 developed to facilitate the quantification of average hydraulic and erosion properties at
531 the field scale (Cerdan et al., 2002a, 2002b).

532 In the WaterSed model, developed in this study, we also used these relationships to
533 compute local water balance and sediment budget, but the application to a 214 km²
534 catchment shows that to only consider the soil surface as the limiting factor that controls
535 hydrological processes is not verified for very wet years. By adding a second limitation,
536 consisting in a distributed soil water capacity limit (filled with rainfall and upslope
537 runoff and emptied with evapotranspiration and percolation), we could reproduce the
538 increase of runoff coefficient during the wettest months. This modification implies to
539 run the model more continuously, as the soil water balance evolves between rainfall
540 events.

541 One first reason to explain the lack of consideration of soil saturation is that most of
542 runoff and soil erosion studies in the European loess belt, are carried out either at the
543 laboratory (rainfall simulation on plots varying from several cm² to several m²) or in the
544 field from the plot to the hillslope scale. On this basis, the scale effects from the plot to
545 the hillslope (or the headwater catchment) scales have been well identified, notably the
546 potential reinfiltration (and sediment deposition) of water when moving downslope

547 explaining the decreasing values of runoff coefficient or sediment erosion rates when
548 moving between these two scales (Cerdan et al., 2004; Cammeraat et al., 2004; Delmas et
549 al., 2012). At the larger catchment scale, emerging processes, such as the contribution of
550 subsurface saturation may need to be taken into account even in the case of well-
551 drained cultivated luvisols of the European Loess belt.

552 A second reason is that model simulations are mostly performed at the rainfall event
553 scale, the effect of saturated conditions can therefore be hidden in the calibration of the
554 hydraulic parameters. For example, a decrease of the infiltration capacity can result in
555 the same model output that a higher infiltration capacity but coupled to limiting soil
556 water capacity if the hydrological conditions do not change too much during the rainfall-
557 runoff event. For runoff and soil erosion simulation at the larger catchment scale (10^2 -
558 10^3 km²), we therefore advise to run a continuous water balance, during, but also
559 between, the rainfall events to properly account for soil saturation.

560 **4. Conclusion**

561 In this study, a unique dataset, including rainfall, discharge, suspended sediment
562 concentration was used to develop and evaluate a runoff and erosion model over 12
563 years. To this end, land use and land cover were also reconstructed together with the
564 corresponding runoff and erosion parameters for this period. The model was applied to
565 a 214 km² catchment located in the Western Paris Basin.

566 In spite of low annual rainfall variability, the inter-annual variability of the runoff
567 volumes and erosion rates at catchment outlets was high. The inter-annual variability of
568 runoff and erosion is closely linked to the number of extreme events per year and their
569 distribution through the year. The model was calibrated on a set of 35 representative
570 rainfall events. The model performed equally well whether saturation-excess runoff was

571 included during the calibration procedure or not, indicating the model robustness but
572 suggesting potential equifinality issue. However, the model was unable to reproduce the
573 runoff dynamics of three wet years included in the dataset if saturation-excess was not
574 included in the model. It suggested that soil surface saturation, a process usually not
575 taken into account when modelling runoff and erosion on cultivated well-drained
576 luvisols of the European loess belts, might be an important process to account for.
577 Interestingly, a seasonal analysis of the results suggested that saturation occurred
578 during most of the modelled period, although sometimes at a limited intensity. The
579 WaterSed model, able to model simultaneously infiltration-excess and saturation-excess
580 runoff, may therefore be an interesting tool to study runoff and erosion in catchments
581 where both processes are expected to occur. Although being a relatively simple model
582 with limited parameters, it demonstrated its ability to model runoff including multiple
583 (in this study, more than 780) rainfall-runoff events. It might therefore be a promising
584 tool to study runoff and erosion across a variety of scale and help identifying the most
585 relevant processes that should be studied further in a variety of context.

586 The first modelling studies in this context had demonstrated the need to use distributed
587 models in order to account for hillslope spatial heterogeneities and redistribution
588 processes (e.g. re-infiltration and deposition processes) at the rainfall event and hillslope
589 scales. The current study brings a complement when moving to larger catchment (10^2 -
590 10^4 km²), pointing to the need to integrate soil saturation processes.

591 **Declaration of competing interest**

592 The authors declare that they have no conflict of interest

593 **Acknowledgements**

594 This research was funded by the AMORAD (ANR-11-RSNR-0002) project (ANR, Agence
 595 Nationale de la Recherche, Programme des Investissements d’Avenir). This work was
 596 also supported by the ANR project “RICOCHET: Multi-risk assessment on coastal territory
 597 in a global change context (2017-2021)” (ANR-16-CE03-0008).

598

599

600

601 **Appendix A – Glossary**

Abbreviation	Unit	Description
e_i	mm.h ⁻¹	Average excess rainfall intensity
ρ	kg.m ⁻³	Bulk density
V_{C_i}	m.s ⁻¹	Channel flow velocity
W_i	m	Channel width
Q_{crit}	m ³ .s ⁻¹	Critical runoff
Q_i	m ³ .s ⁻¹	Cumulative discharge
t_{eff_i}	min	Effective rainfall duration
E_{R_i}	mm	Excess rainfall
L_i	m	Flow length of the cell
A_{G_i}	m ²	Gully cross section
GE_i	kg	Gully erosion
V_{G_i}	m.s ⁻¹	Gully flow velocity
H_{G_i}	m	Gully height
VOL_{G_i}	m ³	Gully volume
W_{G_i}	m	Gully width
HB_i	mm	Hydrologic balance
IR_i	mm	Imbibition rainfall
IE_i	kg	Interrill erosion
n_i	s.m ^{-1/3}	Manning’s roughness coefficient
SD_i	kg	Mass of deposited sediment

SY_{α}	kg	Mass of sediment coming from upslope cells
SY_i	kg	Mass of sediment leaving this cell
WS_i	mm	Maximum water storage
\overline{SC}_i	g.l ⁻¹	Mean suspended sediment concentration of the flow
V_{H_i}	m.s ⁻¹	Overland flow velocity
Δl_i	mm	Potential infiltration for upstream runoff
R_i	mm	Rainfall depth
α	-	Recession parameter
V_{α}	m ³	Runoff coming from upslope cells
T_{R_i}	min	Runoff duration
h_{peak_i}	m	Runoff peak height
Q_{peak_i}	m ³ .s ⁻¹	Runoff peak
V_i	m ³	Runoff volume through a cell
θ	-	Scale effect parameter (0-1)
SC_i	g.l ⁻¹	Sediment concentration in the flow
S_i	m.m ⁻¹	Slope of surface
EF_i	-	Soil erodibility factor
IC_i	mm.h ⁻¹	Steady-state infiltration rate
SC_{TC_i}	g.l ⁻¹	Suspended sediment concentration for the sediment transport capacity
T_{C_i}	min	Time of concentration
TE_i	kg	Total gross erosion

602

603

604

605 **References**

- 606 Aksoy, H., Kavvas, M.L., 2005. A review of hillslope and watershed scale erosion and
607 sediment transport models. *Catena* 64, 247–271.
608 <https://doi.org/10.1016/j.catena.2005.08.008>
- 609 Ballantine, D.J., Walling, D.E., Collins, A.L., Leeks, G.J.L., 2009. The content and storage of
610 phosphorus in fine-grained channel bed sediment in contrasting lowland
611 agricultural catchments in the UK. *Geoderma* 151, 141–149.
612 <https://doi.org/10.1016/j.geoderma.2009.03.021>
- 613 Borrelli, P., Alewell, C., Alvarez, P., Anache, J.A.A., Baartman, J., Ballabio, C., Bezak, N.,
614 Biddoccu, M., Cerdà, A., Chalise, D., Chen, S., Chen, W., De Girolamo, A.M., Gessesse,
615 G.D., Deumlich, D., Diodato, N., Efthimiou, N., Erpul, G., Fiener, P., Freppaz, M.,
616 Gentile, F., Gericke, A., Haregeweyn, N., Hu, B., Jeanneau, A., Kaffas, K., Kiani-
617 Harchegani, M., Villuendas, I.L., Li, C., Lombardo, L., López-Vicente, M., Lucas-Borja,
618 M.E., Märker, M., Matthews, F., Miao, C., Mikoš, M., Modugno, S., Möller, M., Naipal, V.,
619 Nearing, M., Owusu, S., Panday, D., Patault, E., Patriche, C.V., Poggio, L., Portes, R.,
620 Quijano, L., Rahdari, M.R., Renima, M., Ricci, G.F., Rodrigo-Comino, J., Saia, S., Samani,
621 A.N., Schillaci, C., Syrris, V., Kim, H.S., Spinola, D.N., Oliveira, P.T., Teng, H., Thapa, R.,
622 Vantas, K., Vieira, D., Yang, J.E., Yin, S., Zema, D.A., Zhao, G., Panagos, P., 2021. Soil
623 erosion modelling: A global review and statistical analysis. *Sci. Total Environ.* 780.
624 <https://doi.org/10.1016/j.scitotenv.2021.146494>
- 625 Bracken, L.J., Turnbull, L., Wainwright, J., Bogaart, P., 2015. Sediment connectivity: A
626 framework for understanding sediment transfer at multiple scales. *Earth Surf.*
627 *Process. Landforms* 40, 177–188. <https://doi.org/10.1002/esp.3635>
- 628 Cammeraat, E.L.H., 2004. Scale dependent thresholds in hydrological and erosion
629 response of a semi-arid catchment in southeast Spain. *Agric. Ecosyst. Environ.* 104,

- 630 317–332. <https://doi.org/10.1016/j.agee.2004.01.032>
- 631 Cerdan, O., Le Bissonnais, Y., Couturier, A., Bourennane, H., Souchère, V., 2002a. Rill
632 erosion on cultivated hillslopes during two extreme rainfall events in Normandy,
633 France. *Soil Tillage Res.* 67, 99–108. [https://doi.org/10.1016/S0167-](https://doi.org/10.1016/S0167-1987(02)00045-4)
634 [1987\(02\)00045-4](https://doi.org/10.1016/S0167-1987(02)00045-4)
- 635 Cerdan, O., Le Bissonnais, Y., Couturier, A., Saby, N., 2002b. Modelling interrill erosion in
636 small cultivated catchments. *Hydrol. Process.* 3226, 3215–3226.
637 <https://doi.org/10.1002/hyp.1098>
- 638 Cerdan, O., Le Bissonnais, Y., Govers, G., Lecomte, V., Van Oost, K., Couturier, A., King, C.,
639 Dubreuil, N., 2004. Scale effect on runoff from experimental plots to catchments in
640 agricultural areas in Normandy. *J. Hydrol.* 299, 4–14.
641 <https://doi.org/10.1016/j.jhydrol.2004.02.017>
- 642 Cerdan, O., Le Bissonnais, Y., Souchère, V., Martin, P., Lecomte, V., 2002c. Sediment
643 concentration in interrill flow: Interactions between soil surface conditions,
644 vegetation and rainfall. *Earth Surf. Process. Landforms* 27, 193–205.
645 <https://doi.org/10.1002/esp.314>
- 646 Cerdan, O., Souchère, V., Lecomte, V., Couturier, A., Le Bissonnais, Y., 2001. Incorporating
647 soil surface crusting processes in an expert-based runoff model: Sealing and
648 transfer by runoff and erosion related to agricultural management. *Catena* 46, 189–
649 205. [https://doi.org/10.1016/S0341-8162\(01\)00166-7](https://doi.org/10.1016/S0341-8162(01)00166-7)
- 650 Chaplot, V., Le Bissonnais, Y., 2000. Field measurements of interrill erosion under
651 -different slopes and plot sizes. *Earth Surf. Process. Landforms* 25, 145–153.
652 [https://doi.org/10.1002/\(sici\)1096-9837\(200002\)25:2<145::aid-esp51>3.0.co;2-3](https://doi.org/10.1002/(sici)1096-9837(200002)25:2<145::aid-esp51>3.0.co;2-3)
- 653 Chow, V., 1988. *Applied Hydrology*.
- 654 Collins, A.L., Walling, D.E., 2007. Sources of fine sediment recovered from the channel

- 655 bed of lowland groundwater-fed catchments in the UK. *Geomorphology* 88, 120–
656 138. <https://doi.org/10.1016/j.geomorph.2006.10.018>
- 657 De Vente, J., Poesen, J., 2005. Predicting soil erosion and sediment yield at the basin
658 scale: Scale issues and semi-quantitative models. *Earth-Science Rev.* 71, 95–125.
659 <https://doi.org/10.1016/j.earscirev.2005.02.002>
- 660 Delmas, M., Pak, L.T., Cerdan, O., Souchère, V., Le Bissonnais, Y., Couturier, A., Sorel, L.,
661 2012. Erosion and sediment budget across scale: A case study in a catchment of the
662 European loess belt. *J. Hydrol.* 420–421, 255–263.
663 <https://doi.org/10.1016/j.jhydrol.2011.12.008>
- 664 Durán Zuazo, V.H., Rodríguez Pleguezuelo, C.R., 2008. Soil-erosion and runoff prevention
665 by plant covers. A review. *Agron. Sustain. Dev.* 28, 65–86.
666 <https://doi.org/10.1051/agro:2007062>
- 667 Evrard, O., Cerdan, O., van Wesemael, B., Chauvet, M., Le Bissonnais, Y., Raclot, D.,
668 Vandaele, K., Andrieux, P., Biielders, C., 2009. Reliability of an expert-based runoff
669 and erosion model: Application of STREAM to different environments. *Catena* 78,
670 129–141. <https://doi.org/10.1016/j.catena.2009.03.009>
- 671 Evrard, O., Nord, G., Cerdan, O., Souchère, V., Le Bissonnais, Y., Bonté, P., 2010. Modelling
672 the impact of land use change and rainfall seasonality on sediment export from an
673 agricultural catchment of the northwestern European loess belt. *Agric. Ecosyst.*
674 *Environ.* 138, 83–94. <https://doi.org/10.1016/j.agee.2010.04.003>
- 675 Fernandez, C., Wu, J., McCool, D., Stoeckle, C., 2003. Estimating water erosion and
676 sediment yield with GIS, RUSLE, and SEDD. *J. Soil Water Conserv.* 58, 128–136.
- 677 Fu, G., Chen, S., McCool, D.K., 2006. Modeling the impacts of no-till practice on soil
678 erosion and sediment yield with RUSLE, SEDD, and ArcView GIS. *Soil Tillage Res.* 85,
679 38–49. <https://doi.org/10.1016/j.still.2004.11.009>

- 680 Gilley, J.E., Kottwitz, E.R., Wieman, G. a., 1991. Roughness Coefficients for Selected
681 Residue Materials. *J. Irrig. Drain. Eng.* 117, 503–514.
- 682 Gomi, T., Sidle, R.C., Miyata, S., Kosugi, K., Onda, Y., 2008. Dynamic runoff connectivity of
683 overland flow on steep forested hillslopes: Scale effects and runoff transfer. *Water*
684 *Resour. Res.* 44, n/a-n/a. <https://doi.org/10.1029/2007WR005894>
- 685 Govers, G., 1992. Relationship between discharge, velocity and flow area for rills eroding
686 loose, non-layered materials. *Earth Surf. Process. Landforms* 17, 515–528.
687 <https://doi.org/10.1002/esp.3290170510>
- 688 Grangeon, T., Vandromme, R., Pak, L.T., Martin, P., Cerdan, O., Richet, J.B., Evrard, O.,
689 Souchère, V., Auzet, A.V., Ludwig, B., Ouvry, J.F., 2022. Dynamic parameterization of
690 soil surface characteristics for hydrological models in agricultural catchments.
691 *Catena* 214. <https://doi.org/10.1016/j.catena.2022.106257>
- 692 Grimaldi, S., Petroselli, A., Alonso, G., Nardi, F., 2010. Flow time estimation with spatially
693 variable hillslope velocity in ungauged basins. *Adv. Water Resour.* 33, 1216–1223.
694 <https://doi.org/10.1016/j.advwatres.2010.06.003>
- 695 Gumiere, S.J., Le Bissonnais, Y., Raclot, D., Cheviron, B., 2011. Vegetated filter effects on
696 sedimentological connectivity of agricultural catchments in erosion modelling: A
697 review. *Earth Surf. Process. Landforms* 36, 3–19. <https://doi.org/10.1002/esp.2042>
- 698 Hauchard, E., Laignel, B., 2008. Morphotectonic evolution of the north-western margin of
699 the Paris Basin. *Zeitschrift fur Geomorphol.* 52, 463.
- 700 Kronvang, B., Laubel, A., Larsen, S.E., Friberg, N., 2003. Pesticides and heavy metals in
701 Danish streambed sediment. *Hydrobiologia* 494, 93–101.
- 702 Laignel, B., Costa, S., Lequien, a., Massei, N., Durand, a., Dupont, J.P., Bot, L.S., 2008.
703 Current inputs of continental sediment to the English Channel and its beaches: A
704 case study of the cliffs and littoral rivers of the Western Paris Basin. *Zeitschrift für*

- 705 Geomorphol. Suppl. Issues 52, 21–39. <https://doi.org/10.1127/0372->
706 8854/2008/0052S3-0021
- 707 Laignel, B., Dupuis, E., Durand, A., Dupont, J.P., Hauchard, E., Massei, N., 2006. Erosion
708 balance in the watersheds of the western Paris Basin by high-frequency monitoring
709 of discharge and suspended sediment in surface water. *Comptes Rendus - Geosci.*
710 338, 556–564. <https://doi.org/10.1016/j.crte.2006.03.010>
- 711 Laignel, B., Quesnel, F., Meyer, R., Bourdillon, C., 1999. Reconstruction of the Upper
712 Cretaceous chalks removed by dissolution during the Cenozoic in the western Paris
713 Basin. *Int. J. Earth Sci.* 88, 467–474.
- 714 Le Bissonnais, Y., Benkhadra, H., Chaplot, V., Fox, D., King, D., Daroussin, J., 1998.
715 Crusting, runoff and sheet erosion on silty loamy soils at various scales and
716 upscaling from m² to small catchments. *Soil Tillage Res.* 46, 69–80.
717 [https://doi.org/10.1016/s0167-1987\(97\)00079-2](https://doi.org/10.1016/s0167-1987(97)00079-2)
- 718 Le Bissonnais, Y., Cerdan, O., Lecomte, V., Benkhadra, H., Souchère, V., Martin, P., 2005.
719 Variability of soil surface characteristics influencing runoff and interrill erosion.
720 *Catena* 62, 111–124. <https://doi.org/10.1016/j.catena.2005.05.001>
- 721 Le Bissonnais, Y., Renaux, B., Delouche, H., 1995. Interactions between soil properties
722 and moisture content in crust formation, runoff and interrill erosion from tilled
723 loess soils. *Catena* 25, 33–46. [https://doi.org/10.1016/0341-8162\(94\)00040-L](https://doi.org/10.1016/0341-8162(94)00040-L)
- 724 Lyne, V.D., Hollick, M., 1979. Stochastic time-variable rainfall-runoff modeling, in:
725 *Hydrology and Water Resources Symposium, Institution of Engineers Australia,*
726 *Perth.* pp. 89–92.
- 727 Martin, P., 1999. Reducing flood risk from sediment-laden agricultural runoff using
728 intercrop management techniques in northern France. *Soil Tillage Res.* 52, 233–
729 245. [https://doi.org/10.1016/S0167-1987\(99\)00084-7](https://doi.org/10.1016/S0167-1987(99)00084-7)

- 730 Melesse, A.M., Graham, W.D., 2004. Storm runoff prediction based on a spatially
731 distributed travel time method utilizing remote sensing and GIS. *J. Am. Water*
732 *Resour. Assoc.* 40, 863–879. <https://doi.org/10.1111/j.1752-1688.2004.tb01051.x>
- 733 Merritt, W.S., Letcher, R. a., Jakeman, a. J., 2003. A review of erosion and sediment
734 transport models. *Environ. Model. Softw.* 18, 761–799.
735 [https://doi.org/10.1016/S1364-8152\(03\)00078-1](https://doi.org/10.1016/S1364-8152(03)00078-1)
- 736 Moreno-de las Heras, M., Nicolau, J.M., Merino-Martín, L., Wilcox, B.P., 2010. Plot-scale
737 effects on runoff and erosion along a slope degradation gradient. *Water Resour. Res.*
738 46, W04503. <https://doi.org/10.1029/2009WR007875>
- 739 Morgan, R.P.C., 2005. Soil erosion and conservation.
740 <https://doi.org/10.1002/9781118351475.ch22>
- 741 Muzik, I., 1996. GIS Derived Distributed Unit Hydrograph, a New Tool for Flood
742 Modeling. *Water Resour.* 1, 243–247. <https://doi.org/10.4203/ccp.30.10.2>
- 743 Nachtergaele, J., Poesen, J., Sidorchuk, A., Torri, D., 2002. Prediction of concentrated flow
744 width in ephemeral gully channels. *Hydrol. Process.* 16, 1935–1953.
745 <https://doi.org/10.1002/hyp.392>
- 746 Parsons, A.J., Brazier, R.E., Wainwright, J., Powell, M.D., 2006. Scale relationships in
747 hillslope runoff and erosion. *Earth Surf. Process. Landforms* 31, 1384–1393.
748 <https://doi.org/10.1002/esp>
- 749 Patault, E., Ledun, J., Landemaine, V., Soullignac, A., Richet, J.B., Fournier, M., Ouvry, J.F.,
750 Cerdan, O., Laignel, B., 2021. Analysis of off-site economic costs induced by runoff
751 and soil erosion: Example of two areas in the northwestern European loess belt for
752 the last two decades (Normandy, France). *Land use policy* 108, 1–12.
753 <https://doi.org/10.1016/j.landusepol.2021.105541>
- 754 Quesnel, F., Laignel, B., Lefebvre, D., Lautridou, J.P., Lebret, P., 1996. Les formations

- 755 résiduelles à silex de Haute-Normandie. Evolution continentale cénozoïque du NW
756 du Bassin de Paris et utilisation potentielle comme granulats., in: Livret Excursion,
757 In Colloque Géomorphologie et Formations Superficielles, Rouen, 19-21 Mars 1996,
758 BRGM Ed., 248. pp. 65–99.
- 759 Renard, K.G., Foster, G.R., Weesies, G.A., McCool, D.K., Yoder, D.C., 1997. Predicting Soil
760 Erosion by Water: A guide to Conservation Planning With the Revised Universal Soil
761 Loss Equation (RUSLE).
- 762 Robinson, R. a., Sutherland, W.J., 2002. Post-war changes in arable farming and
763 biodiversity in Great Britain. *J. Appl. Ecol.* 39, 157–176.
764 <https://doi.org/10.1046/j.1365-2664.2002.00695.x>
- 765 Shields, F.D., Lizotte, R.E., Knight, S.S., Cooper, C.M., Wilcox, D., 2010. The stream channel
766 incision syndrome and water quality. *Ecol. Eng.* 36, 78–90.
767 <https://doi.org/10.1016/j.ecoleng.2009.09.014>
- 768 Souchère, V., Cerdan, O., Ludwig, B., Le Bissonnais, Y., Couturier, A., Papy, F., 2003.
769 Modelling ephemeral gully erosion in small cultivated catchments. *Catena* 50, 489–
770 505. [https://doi.org/10.1016/S0341-8162\(02\)00124-8](https://doi.org/10.1016/S0341-8162(02)00124-8)
- 771 Souchere, V., King, D., Daroussin, J., Papy, F., Capillon, a., 1998. Effects of tillage on runoff
772 directions: Consequences on runoff contributing area within agricultural
773 catchments. *J. Hydrol.* 206, 256–267. [https://doi.org/10.1016/S0022-](https://doi.org/10.1016/S0022-1694(98)00103-6)
774 [1694\(98\)00103-6](https://doi.org/10.1016/S0022-1694(98)00103-6)
- 775 Stoate, C., Boatman, N.D., Borralho, R.J., Carvalho, C.R., De Snoo, G.R., Eden, P., 2001.
776 Ecological impacts of arable intensification in Europe. *J. Environ. Manage.* 63, 337–
777 365. <https://doi.org/10.1006/jema.2001.0473>
- 778 Tarolli, P., Sofia, G., 2015. Human topographic signatures and derived geomorphic
779 processes across landscapes. *Geomorphology* 255, 140–161.

- 780 <https://doi.org/10.1016/j.geomorph.2015.12.007>
- 781 Van Oost, K., Van Rompaey, A., Poesen, J., Govers, G., Verstraeten, G., 2002. Evaluating an
782 integrated approach to catchment management to reduce soil loss and sediment
783 pollution through modelling. *Soil Use Manag.* 18, 386–394.
784 <https://doi.org/10.1079/SUM2002150>
- 785 Verstraeten, G., Prosser, I.P., Fogarty, P., 2007. Predicting the spatial patterns of hillslope
786 sediment delivery to river channels in the Murrumbidgee catchment, Australia. *J.*
787 *Hydrol.* 334, 440–454. <https://doi.org/10.1016/j.jhydrol.2006.10.025>
- 788 Vigiak, O., Borselli, L., Newham, L.T.H., Mcinnes, J., Roberts, A.M., 2012. Comparison of
789 conceptual landscape metrics to define hillslope-scale sediment delivery ratio.
790 *Geomorphology* 138, 74–88. <https://doi.org/10.1016/j.geomorph.2011.08.026>
- 791 Wainwright, J., 2002. The effect of temporal variations in rainfall on scale dependency in
792 runoff coefficients. *Water Resour. Res.* <https://doi.org/10.1029/2000WR000188>
- 793 Walling, D.E., Owens, P.N., Carter, J., Leeks, G.J.L., Lewis, S., Meharg, A.A., Wright, J., 2003.
794 Storage of sediment-associated nutrients and contaminants in river channel and
795 floodplain systems. *Appl. Geochemistry* 18, 195–220.
- 796 Wang, L., Liu, H., 2006. An efficient method for identifying and filling surface depressions
797 in digital elevation models for hydrologic analysis and modelling. *Int. J. Geogr. Inf.*
798 *Sci.* 20, 193–213. <https://doi.org/10.1080/13658810500433453>
- 799 Wilcox, B.P., Breshears, D.D., Allen, C.D., 2003. Ecohydrology of a resource- conserving
800 semiarid woodland: Effects of scaling and disturbance. *Ecol. Monogr.* 73, 223–239.
- 801 Yair, A., Raz-Yassif, N., 2004. Hydrological processes in a small arid catchment: Scale
802 effects of rainfall and slope length. *Geomorphology* 61, 155–169.
803 <https://doi.org/10.1016/j.geomorph.2003.12.003>

Declaration of interests

The authors declare that they have no known competing financial interests or personal relationships that could have appeared to influence the work reported in this paper.

The authors declare the following financial interests/personal relationships which may be considered as potential competing interests:

Journal Pre-proof